

Wet oxidation of GeSi at 700 °C

W. S. Liu, E. W. Lee,^{a)} and M-A. Nicolet
California Institute of Technology, Pasadena, California 91125

V. Arbet-Engels and K. L. Wang
University of California, Los Angeles, California 90024

N. M. Abuhadba and C. R. Aita
Materials Department, University of Wisconsin-Milwaukee, Milwaukee, Wisconsin 53201

(Received 9 December 1991; accepted for publication 13 January 1992)

About 500-nm-thick films of $\text{Ge}_{0.36}\text{Si}_{0.64}$ and $\text{Ge}_{0.28}\text{Si}_{0.72}$ grown epitaxially on (100)Si have been oxidized at 700 °C in wet ambient. A uniform $\text{Ge}_x\text{Si}_{1-x}\text{O}_2$ oxide layer forms with a smooth interface between it and the unoxidized $\text{Ge}_x\text{Si}_{1-x}$ layer below. The composition and structure of that layer remains unchanged as monitored by backscattering spectrometry or cross-sectional transmission electronic microscopy. The oxide of both samples grows as square root of oxidation duration. The parabolic rate constant increases with the Ge content and is larger than that for wet oxidation of pure Si at the same temperature. The absence of a regime of linear growth at this relatively low temperature indicates a much enhanced linear rate constant.

I. INTRODUCTION

The oxidation of $\text{Ge}_x\text{Si}_{1-x}$ has been studied by several authors using conventional and high pressure furnace as well as rapid thermal processing.¹⁻¹⁰ Initially it was reported that for GeSi samples of low Ge content ($x < 0.2$) a pure SiO_2 layer grows with Ge piling up behind it.¹⁻⁶ However, Ge can also be oxidized to form a GeSi oxide when the Si supply at the reaction interface is insufficient. This was observed at low temperature (< 700 °C)^{9,10} or in high Ge content cases.^{7,8} The oxidation rate is larger than that of pure Si whether Ge is oxidized or piles up behind the oxide.⁷ The wet oxidation of GeSi at low temperature is especially interesting because of the very large oxidation rate, the uniform GeSi oxide formed,⁹ and the consequent low thermal budget of the process. We present here the kinetics of the oxidation of epitaxial $\text{Ge}_x\text{Si}_{1-x}$ samples of two different Ge contents at 700 °C in wet ambient. The oxide structure is also investigated by transmission electron microscopy, backscattering spectrometry, and infrared spectrometry.

II. EXPERIMENT

The GeSi samples for this study were grown epitaxially onto (100)Si substrates by molecular beam epitaxy without intentional doping. One sample is a layer of $\text{Ge}_{0.36}\text{Si}_{0.64}$ about 470 nm thick, the other layer of $\text{Ge}_{0.28}\text{Si}_{0.72}$ about 550 nm thick. Both films are elastically relaxed as determined from x-ray double-crystal diffractometry. The large thickness was chosen to ensure that the oxide would never reach the substrate under the conditions of our experiments.

The oxidation was done in a tube furnace at 700 °C in wet ambient obtained by bubbling nitrogen gas through

95 °C de-ionized water. The samples were exposed to the oxidant ambient only after they had reached the desired temperature to avoid oxidation during the heating transient of the samples.¹¹ For this purpose, the tube was flushed with nitrogen for approximately 1 h before oxidation. The samples were then introduced into the furnace. After about 10 min, the furnace atmosphere was switched from pure nitrogen to wet nitrogen.

III. RESULT

A. Backscattering spectrometry results

Figures 1(a) and 1(b) show the backscattering spectra of the two $\text{Ge}_x\text{Si}_{1-x}$ samples before and after they were oxidized at 700 °C for 1 h. It is clear that in both cases the oxide includes Ge which is uniformly distributed in depth. Within the resolution of backscattering spectrometry, no germanium is lost in both cases. The composition of the oxide derived from the backscattering spectrum of the $\text{Ge}_{0.36}\text{Si}_{0.64}$ sample is $\text{Ge}_{0.35}\text{Si}_{0.65}\text{O}_2$ with an error of $\pm 5\%$. The Ge:Si ratio in the oxide differs insignificantly from that of the original epilayer. A similar result holds for the $\text{Ge}_{0.28}\text{Si}_{0.72}$ sample. No pileup of Ge or Si is seen behind the oxide and the oxide structure is x-ray amorphous in both cases. These facts prove that the Ge and Si in the GeSi layer are fully oxidized simultaneously. The composition of the oxide is consistent with that of a mixture of SiO_2 and GeO_2 . For the same 1 h duration of oxidation, the oxide of $\text{Ge}_{0.36}\text{Si}_{0.64}$ sample is about 1.4 times thicker than that of the $\text{Ge}_{0.28}\text{Si}_{0.72}$ sample, as follows from a comparison of the area of the two oxygen signals in the spectra.

B. Structure characterization

Figure 2 shows a cross-sectional transmission electron micrograph of the $\text{Ge}_{0.36}\text{Si}_{0.64}$ sample after oxidation at 700 °C for 1 h. Two distinct uniform layers are clearly seen. The thickness of the oxide varies laterally by about 10%;

^{a)}Permanent address: Department of Physics, Kyungpook National University, Taegu, Korea.

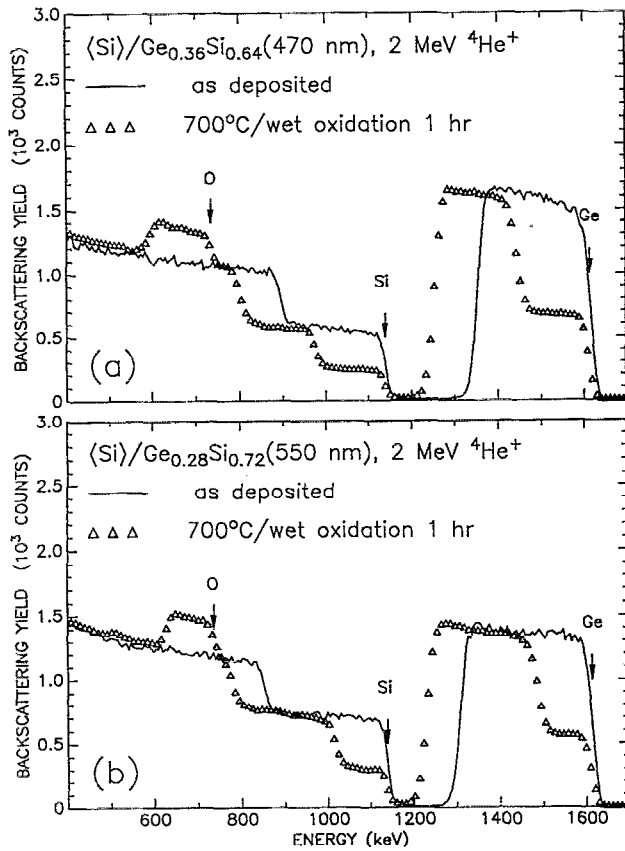


FIG. 1. 2 MeV $^4\text{He}^+$ backscattering spectra of epitaxial layers of (a) $\text{Ge}_{0.36}\text{Si}_{0.64}$, (b) $\text{Ge}_{0.28}\text{Si}_{0.72}$ on (100)Si before and after oxidation for 1 h in wet ambient at 700 °C, showing a uniform composition of the GeSi oxide. The scattering angle of detected particles is 170°.

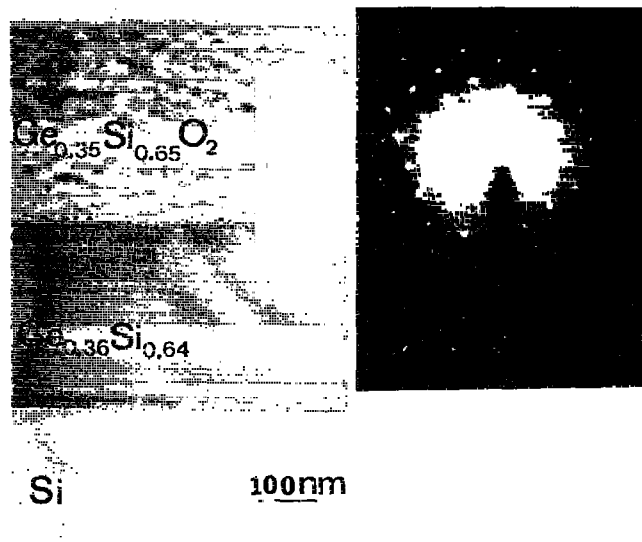


FIG. 2. Cross-sectional transmission electron micrograph of GeSi oxide/GeSi layer for $\text{Ge}_{0.36}\text{Si}_{0.64}$ after oxidation at 700 °C for 1 h, showing the smooth GeSi oxide/GeSi layer interface. The diffraction pattern that samples both the oxidized and the unoxidized GeSi layer is also inserted.

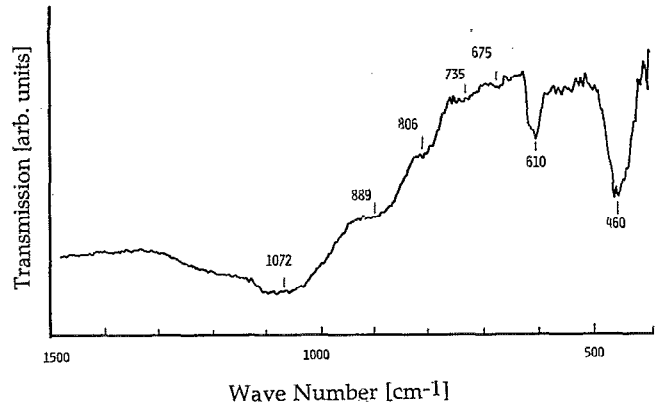


FIG. 3. Infrared transmission as a function of wave number for an oxidized $\text{Ge}_{0.36}\text{Si}_{0.64}$ layer.

that of the remaining unoxidized GeSi layer is laterally constant. Included in the figure is a transmission electron diffraction pattern obtained with a beam that was probing both the oxidized and the unoxidized GeSi layers. The transmission electron diffraction pattern contains diffuse rings characteristic of a noncrystalline structure which originates from the oxide layer as was established by independent diffraction experiments. The remaining unoxidized $\text{Ge}_{0.36}\text{Si}_{0.64}$ layer is still single crystalline by electron diffraction. There is no indication of a region with a changed Ge content in the remaining GeSi layer as Ge pileup would produce. The cross-sectional transmission electron micrograph of the sample with only 28 at. % Ge for oxidation at 700 °C for 1 h shows a similar structure but with a thinner oxide (about 240 nm) than that of the sample with 36 at. % Ge (about 340 nm). From these oxide thicknesses and the corresponding backscattering data, we calculate the density of $\text{Ge}_{0.36}\text{Si}_{0.64}\text{O}_2$ and $\text{Ge}_{0.28}\text{Si}_{0.72}\text{O}_2$ to be 2.1×10^{22} formula units/cm³, with an estimated error of 10%. This density is similar to that of amorphous SiO_2 (2.25×10^{22} molecules/cm³).

To test the oxidation state of the layer, a $\text{Ge}_{0.36}\text{Si}_{0.64}$ sample was oxidized at 700 °C for 48 h which completely consumed the GeSi layer and also some of the substrate Si. A Nicolet model MX-1 Fourier transform infrared spectrometer was used to obtain infrared absorption spectra of the layer. The instrument was calibrated to an accuracy of $\pm 4 \text{ cm}^{-1}$ using a polystyrene standard. A spectrum taken between 400 and 1500 cm^{-1} (25.0 and 6.7 μm) is shown in Fig. 3. The absorption peak assignment is as follows:^{12,13} SiO_2 features characteristic of the quartz-derived bonding of $[\text{SiO}_4]$ tetrahedra in melt-quenched SiO_2 glass include major peaks at 460 cm^{-1} , attributed to Si-O bending, and 1072 cm^{-1} , attributed to Si-O stretching. Minor peaks at 675 and 806 cm^{-1} are attributed to Si stretching. In addition, a peak at 610 cm^{-1} is attributed to Si stretching in $[\text{SiO}_4]$ tetrahedra bonded in a manner characteristic of crystalite, another modification of SiO_2 .

GeO_2 crystallizes in two forms: a hexagonal form analogous to quartz in which $[\text{GeO}_4]$ tetrahedra are the building blocks, and a tetragonal rutile form in which the basic

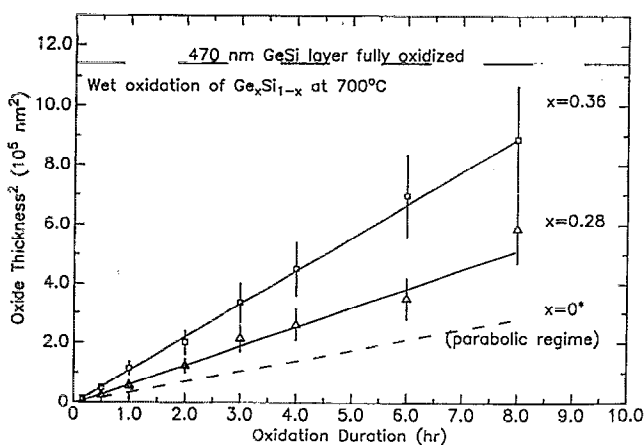


FIG. 4. Square of the oxide thickness vs the duration of wet oxidation for the $\text{Ge}_{0.36}\text{Si}_{0.64}$ and $\text{Ge}_{0.28}\text{Si}_{0.72}$ samples. The solid straight lines through the origin indicate a pure parabolic growth.

units are $[\text{GeO}_6]$ octahedra. Short-range order characteristic of both coordinations is observed here. The major GeO_2 peak at 889 cm^{-1} is attributed to Ge-O stretching in $[\text{GeO}_4]$ tetrahedra. In addition, a small peak at 735 cm^{-1} is attributed to Ge-O stretching in $[\text{GeO}_6]$ octahedra.

The oxides of our two samples appear quite similar in the cross-sectional transmission electron micrographs. This is noteworthy because in the SiO_2 - GeO_2 quasi-binary phase diagram¹⁴ at 700°C GeO_2 (which has the tetragonal rutile structure) is soluble in SiO_2 (which has the hexagonal β -quartz structure) up to a limit of 32% only. No such boundary exists between 28% and 36% in the amorphous phase, probably because much of the Ge is tetrahedrally bonded in the same way Si is, as the infrared spectra show.

C. Kinetics

The square of the oxide thickness, calculated from backscattering spectra and the known density of the oxides, versus oxidation duration at 700°C is shown in Fig. 4 for the $\text{Ge}_{0.36}\text{Si}_{0.64}$ sample and $\text{Ge}_{0.28}\text{Si}_{0.72}$ sample. All oxidized samples have spectra similar to those of Fig. 1 reflecting a uniform oxide composition, but with different thicknesses. The oxidation of both samples can be expressed by a parabolic growth law as can be seen from Fig. 4 where the square of the oxide thickness is plotted linearly with the oxidation duration. The parabolic rate constant is $1.1 \times 10^5 \text{ nm}^2/\text{h}$ for the $\text{Ge}_{0.36}\text{Si}_{0.64}$ sample and $6.4 \times 10^4 \text{ nm}^2/\text{h}$ for the $\text{Ge}_{0.28}\text{Si}_{0.72}$ sample. The latter one is still larger than that for wet oxidation of pure Si ($4 \times 10^4 \text{ nm}^2/\text{h}$, which is also plotted in the figure as the dashed line) extrapolated from Deal and Grove's paper.¹⁵ However, at this temperature, the oxide growth of pure Si in wet ambient actually follows the linear law within this range of oxide thicknesses.

IV. DISCUSSION

Oxidation consists of two major processes: reaction and diffusion, the slower one of which determines the kinetics of oxidation. Regarding the diffusion process, no

direct determination of the moving species during thermal oxidation of Ge or $\text{Ge}_x\text{Si}_{1-x}$ alloys has been reported in the literature for either wet or dry ambients. Law and Meigs¹⁶ assume that Ge moves in the oxidation of Ge, following the behavior observed in most metals, but experiments by Crisman *et al.*¹⁷ later provided strong evidence to the contrary. For Si, it is well established that the oxidant is the moving species for both wet and dry ambients in both the linear and the parabolic regimes.^{18,19}

In our study, a uniform oxide is formed with a smooth oxide/semiconductor interface. If the oxidant were not the moving species, Ge and Si would have to both diffuse and in such manner that even for different diffusivities in the oxide, their fluxes toward the surface would have to be equal to keep the oxide composition uniform as it is observed to be. In addition, this would have to be true for different compositions of the oxide, as our experiments show. Although we cannot exclude this possibility, we consider it very unlikely. Most probably it is the oxidant that moves, so that the reaction occurs at the interface as in the case for pure Si. A definitive proof of this conclusion has to be carried out with a marker experiment.

A parabolic growth as observed in Fig. 4 indicates a diffusion-limited process. We thus compare our results with those of Si and Ge in their parabolic growth regimes. Our $\text{Ge}_x\text{Si}_{1-x}$ epilayers show a larger parabolic constant than pure Si (Fig. 4). We cannot compare directly with Ge because wet oxidation data do not seem to exist in the literature. Dry oxidation of Ge, however, has been reported to be parabolic at 550 , 575 , and 600°C .^{20,21} Extrapolating their data to 700°C , the parabolic rate constant surpasses that measured here for GeSi. Presumably, the wet oxidation of Ge will be much larger yet. The parabolic rate constants measured here thus fall between those of pure Si and Ge. We recall that the sample with 36% oxidizes 1.4 times faster than that with 28% Ge. It thus appears that increasing the GeO_2 content in the oxide also raises the parabolic constant. This can be attributed to an enhanced diffusivity and/or an increased water solubility in $\text{Ge}_x\text{Si}_{1-x}\text{O}_2$.

Our GeSi oxide shows a uniform composition throughout the oxide thickness (Fig. 1). That is so even when the whole GeSi layer is completely oxidized (about $1.1 \mu\text{m}$ oxide). This is different from the previous oxidation studies of GeSi. In cases where $x > 0.5$,^{7,8} although Ge oxidizes initially, it is excluded from the oxidation afterwards and only SiO_2 forms subsequently. In other cases where $x < 0.5$ ¹⁻⁸ only SiO_2 forms from the start and Ge immediately piles up behind the growing oxide. To compare the present results with others published so far, one should notice that all previous studies were performed at 800°C and above while here the temperature is 700°C . At such a low temperature, the diffusive transport of Si and Ge in the epilayer is frozen.⁹ This is why the Si:Ge ratio remains constant in space and time in the present case. In this limiting case, the oxidation of $\text{Ge}_x\text{Si}_{1-x}$ proceeds as it would for an elemental material.

Pure Si at 700°C , however, oxidizes linearly in time within the range of oxide thicknesses observed here. We see

no such linear growth regime. The rate constant for the oxidation reaction of $\text{Ge}_x\text{Si}_{1-x}$ hence must be substantially higher than it is for pure Si. In fact, the reaction rate constant for $\text{Ge}_x\text{Si}_{1-x}$ must be increased by a factor which exceeds that by which the parabolic rate constant rises because otherwise, the growth law would be linear, as it is in pure Si. Several causes can be advanced for such an enhancement of the reaction rate constant. The stable crystalline phase of GeO_2 is that of rutile which is sixfold coordinated. Upon oxidation Ge thus changes coordination while Si does not because it forms the fourfold coordinated quartz. This change in coordination for Ge can enhance the reaction rate. That explanation is unlikely, however, because much of the Ge is fourfold coordinated in the amorphous $\text{Ge}_x\text{Si}_{1-x}\text{O}_2$. Another possible cause is the increased free charge carrier concentration resulting from the reduced band gap of $\text{Ge}_x\text{Si}_{1-x}$. In the case of silicides, it is well established that the semiconducting silicides have a reduced linear reaction rate constant compared to that of the metallic silicides.²² Yet another possible cause is the local strain that must exist in the $\text{Ge}_x\text{Si}_{1-x}$ alloy as a result of the random microscopic heterogeneities. This hypothesis suggests an experiment to compare the linear rate of oxidation for epitaxial films with different elastic strains at constant composition.

V. CONCLUSION

The ability to form a uniform oxide with a sharp oxide/semiconductor interface at relatively low temperature is potentially very significant for the $\text{Ge}_x\text{Si}_{1-x}$ technology, providing that the oxide is stable, has a high dielectric strength, and can passivate the $\text{Ge}_x\text{Si}_{1-x}$ surface. The present study establishes that a low-temperature oxide growth is possible. The properties of the resulting $\text{Ge}_x\text{Si}_{1-x}\text{O}_2$ films will decide whether the oxide is also useful. The next effort should thus aim at determining the properties of $\text{Ge}_x\text{Si}_{1-x}\text{O}_2$.

ACKNOWLEDGMENTS

This work was supported by the Semiconductor Research Corporation under a coordinated research program

between Caltech (91-SJ-100) and at UCLA (91-SJ-088). We thank Dr. W. A. Goddard for a useful discussion, J. S. Chen for the transmission electron microscopy study, and R. Gorris for his technical assistance. E. W. Lee acknowledges the support of the Korean Ministry of Education.

- ¹O. W. Holland, C. White, and D. Fathy, *Appl. Phys. Lett.* **51**, 520 (1987).
- ²D. Fathy, O. W. Holland, and C. White, *Appl. Phys. Lett.* **51**, 1337 (1987).
- ³F. K. LeGoues, R. Rosenberg, T. Nguyen, F. Himpsel, and B. S. Meyerson, *J. Appl. Phys.* **65**, 1724 (1989).
- ⁴F. K. LeGoues, R. Rosenberg, and B. S. Meyerson, *Appl. Phys. Lett.* **54**, 644 (1989).
- ⁵D. Nayak, K. Kamjoo, J. C. S. Woo, J. S. Park, and K. L. Wang, *Appl. Phys. Lett.* **56**, 66 (1990).
- ⁶D. K. Nayak, K. Kamjoo, J. S. Park, J. C. S. Woo, and K. L. Wang, *Appl. Phys. Lett.* **57**, 369 (1990).
- ⁷J. Eugene, F. K. LeGoues, V. P. Kesan, S. S. Iyer, and F. M. d'Heurle, *Appl. Phys. Lett.* **59**, 78 (1991).
- ⁸H. K. Liou, P. Mei, U. Gennser, and E. S. Yang, *Appl. Phys. Lett.* **59**, 1200 (1991).
- ⁹W. S. Liu, G. Bai, M-A. Nicolet, C. H. Chern, V. Arbet, and K. L. Wang, *Mater. Res. Soc. Symp. Proc.* **220**, 259 (1991).
- ¹⁰D. C. Paine, C. Caragianis, and A. F. Schwartzman, *J. Appl. Phys.* **70**, 5076 (1991).
- ¹¹W. S. Liu, E. W. Lee, M-A. Nicolet, V. Arbet-Engels, and K. L. Wang, *J. Appl. Phys.* (to be published).
- ¹²E. R. Lippincott, A. Van Valkenburg, C. E. Weir, and E. N. Bunting, *J. Res. NBS* **61**, 61 (1958).
- ¹³K. Suzuki, *Diff. Defect Data* **53-54**, 233 (1987).
- ¹⁴E. C. Shafer and R. Roy, U.S. Army Signal Corps Contract DA 36-039, SC 63099, 1956.
- ¹⁵B. E. Deal and A. S. Grove, *J. Appl. Phys.* **36**, 3770 (1965).
- ¹⁶J. T. Law and P. S. Meigs, *J. Electrochem. Soc.* **104**, 154 (1957).
- ¹⁷E. E. Crisman, Y. M. Ercil, J. J. Loferski, and P. J. Stiles, *J. Electrochem. Soc.* **128**, 1845 (1982).
- ¹⁸J. R. Ligenza and W. G. Spitzer, *J. Phys. Chem. Solids* **14**, 131 (1960).
- ¹⁹P. J. Jorgensen, *J. Chem. Phys.* **37**, 784 (1962).
- ²⁰J. Sladkova, *Czech. J. Phys. B* **18**, 801 (1968).
- ²¹J. Sladkova, *Czech. J. Phys. B* **27**, 943 (1977).
- ²²F. M. d'Heurle, R. D. Frampton, E. A. Irene, H. Jiang, and C. S. Petersson, *Appl. Phys. Lett.* **47**, 1170 (1985).